Northern Blot Analysis

Total RNA (10 μg) extracted from each cell was analyzed using the Ambion Northernmax Kit (Life Technologies) according to the manufacturer's guidelines. Hybridization was performed under standard conditions with a digoxigenin-labeled human CYGB cDNA probe. The final washing conditions were 65 °C at 0.1× standard saline citrate (SSC). The blot filter was exposed for 24 h using Kodak XROmat film.

Immunoblot Analysis

Immunoblot analysis for CYGB protein detection was performed essentially as described previously [36] using rabbit anti-CYGB antibody, a kind gift from Dr. Norifumi Kawada [8], and β-actin antibody (Cell Signaling Technology, Beverly, MA). The images were obtained using ImageQuant LAS 3000 (Fujifilm, Tokyo, Japan).

Immunohistochemical Analysis

A skin tumor tissue array (T212a) including normal tissue as a control was purchased from Biomax US (Rockville, MD) and was analyzed as described previously [37] using the rabbit anti-CYGB antibody, and a mouse antibody against PNL2 (Cell Marque, Rocklin CA), a highly specific marker for melanoma and melanocyte.

Immunofluorescence Staining

To detect CYGB expression in melanocyte and melanoma cell lines, cells grown to subconfluence on cover slips were rinsed with PBS and fixed in 4% formaldehyde for 30 min at room temperature (RT). After rinsing several times with PBS, cells were blocked with 10% goat serum for 30 min and were incubated in PBS containing anti-CYGB antibody (1:200) for 1 hour at RT. Cells were then washed with PBS and incubated in PBS containing 10 μg/mL of Alexa Fluor 488 goat anti-rabbit IgG (Molecular Probes, Eugene, OR). After washing 3 times in PBS, the cover slips were mounted on a slide glass using Vectashield (Vector Laboratories, Burlingame, CA). The images were captured using a fluorescence microscope (IX71; Olympus, Tokyo, Japan).

CYGB Promoter Methylation Analysis

Genomic DNA was extracted from the G361 and A375 cell lines and melanocytes using Blood & Cell Culture DNA Kits (Qiagen, Hilden, Germany). Bisulfite treatment for each sample (0.8 μg) was performed using the CpGenome Turbo Bisulfite Modification Kit (Millipore, Billerica MA). The modified DNA was subjected to PCR amplification using NovaTaq DNA Polymerase (Merk, Darmstadt, Germany) and primers that were designed to exclude the CpG site, thereby rendering the amplification independent of the methylation status. The primer sequences were as follows: 5′-GGGAATTGATTTAAAGTT-TAAT-3′ (forward), and 5′-TAACCCCCCAAACCTAA-3′ (Reverse). The DNA sequencing of the amplicon (matching GenBank accession NC_000017.10) was performed in both directions using the BigDye Terminator v3.1 Cycle Sequencing Kit (Applied Biosystems).

siRNA Transfection

siRNA targeting human CYGB and negative control siRNA were purchased from Qiagen. The targeting sequences for CYGB and control (scrambled sequence) siRNA were 5′-GGA GGA AUC CCU GAC UCA A-3′ and 5′- GAG CAG UCC CAU CGA UAG A -3′; respectively. The transfection methods have been described previously [38].

Short Hairpin RNAs (shRNAs) Transfection

Targeting sequences used to construct shRNA for human CYGB and nonsilencing control (scrambled sequence) were same as siRNA sequences. They were cloned into an RNAi-Ready pSIREN-RetroQ-ZsGreen vector (Clontech) according to manufacturer's protocol. The stable transfectants of G361 cells expressing these shRNAs were obtained as previously described [38].

Xenogtrafts in Nude Mice

Assay of tumor in nude mice (BALB/c-nu/nu, 5–8 wk old females; CLEA Japan Inc., Tokyo, Japan) was performed as described previously [39] in strict accordance with the recommendations for the Handling of Laboratory Animals for Biomedical Research, as documented by the Institutional Animal Care and Use Committee (IACUC) at the Kinki University Faculty of Medicine (Permit Number: KAME-24-005). The stable transfectants of G361 cells expressing CYGB and control shRNAs were suspended in PBS and Matrigel (BD Biosciences) (1:1) at a density of 1×10^7 cells/ml. One million cells were injected subcutaneously into the interscapular region of mice (n = 5). Tumor size was assessed at 3 to 4-day interval and the tumor volume V was calculated according to the formula: $V = W^2\times L\times0.5$, where W and L are tumor width and length, respectively. At the end of the experiment, the mice were killed and the xenografts were resected, fixed in 10% buffered formalin for 10 h, and processed for histological analysis. Apoptosis was determined by immunohistochemistry using anti-cleaved caspase 3 antibody (Cell Signaling Technology) as previously described [39].

Cell Proliferation Assay

Cell proliferation was assessed using an MTT assay, as described previously [36].

Measurement of ROS Production

Cells were transfected with CYGB siRNA or control siRNA and ROS generation was detected using 2′-, 7′-dichlorofluorescein diacetate (DCFH-DA) (Invitrogen). The cells were incubated with 10 μM of DCFH-DA for 30 min at 37°C and washed twice with PBS. After trypsinization, the cells were immediately analyzed using a FACScan flow cytometer (BD Biosciences, San Jose, CA).

Assessment of Cell Death

Cell death was analyzed by staining the cells using an annexin V-FITC apoptosis detection kit I (BD Pharmingen, San Diego, CA), a procedure that reveals both apoptosis and necrosis. Briefly, G361 cells were transfected with CYGB siRNA or control siRNA and were treated with or without 100 μM H_2O_2 for 24 hours. After trypsinization followed by washing in PBS, the cells (1×10^5) were resuspended in 100 μL binding buffer, to which FITC-Annexin and propidium iodide (PI) have been added, and incubated for 15 min. Cell death was measured using a flow cytometer.

Statistical Analysis

The statistical analyses were performed using Microsoft Excel to calculate the SE and to test for statistically significant differences between the samples using the Student *t* test. A *P* value of <0.05 was considered statistically significant.

Supporting Information

Figure S1 *CYGB* mRNA is abundantly expressed in some melanoma cells. A. Northern blot analysis of *CYGB* mRNA in A549, T47D, T98G and 5 melanoma cells under normoxic (N) and anoxic (0.1%–0.2% O_2) (A) conditions. β-actin was used as a loading control. **B.** The relative CYGB expression levels that were assessed by realtime quantitative PCR using TaqMan probes and were compared with 18S rRNA expression are listed for the same cells as those analyzed in A. SEM values are shown in parenthesis.
(TIF)

Figure S2 CYGB is predominantly distributed in melanocytes within the skin. A. Immunoblot analysis of CYGB protein in NHDF, keratinocytes and melanocytes from skin and 8 melanoma cell lines (WM35 to HS294T). The image was obtained using ImageQuant LAS 3000 with an exposure time of 120 sec. **B.** Immunocytochemistry analysis of melanocytes, G361 and A375 cells using CYGB antibody. Scale bar, 5 μm.
(TIF)

Figure S3 *CYGB* mRNA expression is reduced in most melanoma tissues during melanocyte-to-melanoma transition. *CYGB* mRNA expression was compared in eight melanocyte cell lines (shown as red bars) and melanoma tissues from 82 patients deposited in the GSE29359 GEO dataset. The bar chart was drawn based on the meta-analysis described in the legend to Table S4. A horizontal line is drawn to show tissues with a relatively high expression of CYGB (higher than 0.3).
(TIF)

Figure S4 *CYGB* mRNA expression is inversely correlated with the methylation status. The GSE28356 GEO dataset with a platform of Illumina HumanMethylation27 BeadChip was meta-analyzed for the methylation status of the CYGB gene promoter (gene ID cg17040807) in 9 melanoma cell lines and one melanocyte pool, which was used as a normalization control. The beta value that indicated a continuous, quantitative measurement of DNA methylation, ranging from 0 (completely unmethylated) to 1 (completely methylated), was used for the calculation. The expression of cytoglobin mRNA was estimated using the GSE7152 dataset that analyzed 35 melanoma cell lines with an Affymetrix expression microarray platform. The probesets for cytoglobin mRNA (1553572_a_at) and GAPDH mRNA (M33197_M_at), a normalization control, were used. The nine cells analyzed in common to both datasets are listed **(A)** and compared for their normalized levels of the CYGB expression and *CYGB* promoter methylation **(B)**.
(TIF)

Figure S5 Efficacy of shRNA-mediated CYGB knockdown in G361 cells. G361 cells stably expressing shRNA against CYGB and control shRNA were generated by retrovirus transduction. **A.** Confirmation of CYGB knockdown in the cell line expressing CYGB shRNA at the protein level by Western analysis. β-actin was used as a loading control. **B.** Growth analysis of CYGB knockdown in G361 cells. G361 cells expressing CYGB shRNA and control shRNA were seeded in 96 well plates (2,000 cells/well) and cell growth was determined by MTT assay. OD value, 570 nm. bars, SEM. * $P<0.05$, ** $P<0.01$. **C.** Immunohistochemistry pictures of cleaved caspases 3-positive cells in G361 xenografts (Scale bar, 100 μm). **D.** Quantification of the apoptosis-signal in C ($P<0.01$, mean ± SD, $n = 5$).
(TIF)

Table S1 Cell lines used in the experiment and their origins. The list covers the cell lines analyzed by immunoblotting (Fig. 1) and northern blotting (Fig. 2*A*). The other cell lines subjected to preliminary screening using northern blotting included the following: H69, PC14, H1299, A427, Calu1, H520, H460, H1650, PC-9, H1975 (lung cancer), SKBR3, MDA-MB-468, MDA-MB-231, BT549, HCC1954 (breast cancer), Colo201, HCT116, WiDr, LoVo, SW480 (colon cancer), MKN1, IM95, MKN7, SNU1 (gastric cancer), LnCAP, Du145 (prostatic cancer), SCOV3, OVCAR3 (ovarian cancer), Caki-1, RCC4 (renal cell carcinoma), BxPC3, Capan1 (pancreatic cancer), A172, U87 (glioblastoma) and Hep3B (hepatoma), all of which gave no positive signal for CYGB.
(DOC)

Table S2 Expression of cytoglobin mRNA in cell lines from several cancer types (1). The GSE10843 GEO dataset with an Affymetrix expression microarray platform (GeneChip, HG-U133_Plus_2) was meta-analyzed for the expression of cytoglobin mRNA using 1553572_a_at, a transcript ID for cytoglobin. A transcript of glyceraldehyde 3-phosphate dehydrogenase (GAPDH; M33197_M_at) was used as a normalization control. To make the expression ratios comparable, the normalized CYGB/GAPDH value for MEWO melanoma cell line was set equal to 1. The database included 118 cell lines consisting of 15 melanoma (highlighted in red), 12 breast cancer, 50 lung cancer, 9 ovarian cancer, 6 lymphoma, and 26 colon cancer cell lines. The samples were aligned according to the order of the normalized expression level of *CYGB* mRNA.
(XLS)

Table S3 Expression of cytoglobin mRNA in cell lines from several cancer types (2). Several GEO datasets with an Affymetrix expression microarray platform (GeneChip) were used for the meta-analysis of cytoglobin mRNA expression (1553572_a_at) and a GAPDH mRNA (M33197_M_at) as a normalization control. To make the expression ratios comparable for all cell lines listed in both Tables S2 and S3, the normalized CYGB/GAPDH value for MEWO, which was set equal to 1 in Table S2, was introduced. The five datasets, GSE8332, GSE17714, GSE22563, GSE15455, and GSE9171, included 20 pancreatic, 11 neuroblastoma, 11 renal cell carcinoma, 33 gastric, and 17 glioblastoma cell lines, respectively. The samples with relatively abundant *CYGB* mRNA are highlighted.
(XLS)

Table S4 Expression of cytoglobin mRNA in eight melanocyte cell lines and melanoma tissues from 79 patients. The GSE29359 GEO dataset with an Ilumina expression microarray platform (beadarray) was meta-analyzed for the expression of cytoglobin mRNA using ILMN_1758128, a transcript ID for cytoglobin. A GAPDH transcript (ILMN_2038778) was used as a normalization control. The melanoma samples were aligned according to the order of the normalized expression level of CYGB mRNA. Three patients (62, 64 and 82) with poor GAPDH expression values were excluded from the comparison.
(DOC)

Acknowledgments

We thank Tomoko Kitayama for the *in vivo* work, Yoshihiro Mine for the sequencing, and Shinji Kurashimo for the flow cytometry studies.

Author Contributions

Conceived and designed the experiments: YF SK KN. Performed the experiments: YF SK MD YT TM. Analyzed the data: YF SK JB. Contributed reagents/materials/analysis tools: MT HH. Wrote the paper: YF MD KN.

References

1. Burmester T, Ebner B, Weich B, Hankeln T (2002) Cytoglobin: a novel globin type ubiquitously expressed in vertebrate tissues. Mol Biol Evol 19: 416–421.
2. Pesce A, Bolognesi M, Bocedi A, Ascenzi P, Dewilde S, et al. (2002) Neuroglobin and cytoglobin. Fresh blood for the vertebrate globin family. EMBO Rep 3: 1146–1151.
3. Oleksiewicz U, Liloglou T, Field JK, Xinarianos G (2011) Cytoglobin: biochemical, functional and clinical perspective of the newest member of the globin family. Cell Mol Life Sci 68: 3869–3883.
4. Kawada N, Kristensen DB, Asahina K, Nakatani K, Minamiyama Y, et al. (2001) Characterization of a stellate cell activation-associated protein (STAP) with peroxidase activity found in rat hepatic stellate cells. J Biol Chem 276: 25318–25323.
5. Xu R, Harrison PM, Chen M, Li L, Tsui TY, et al. (2006) Cytoglobin overexpression protects against damage-induced fibrosis. Mol Ther 13: 1093–1100.
6. Fordel E, Thijs L, Martinet W, Lenjou M, Laufs T, et al. (2006) Neuroglobin and cytoglobin overexpression protects human SH-SY5Y neuroblastoma cells against oxidative stress-induced cell death. Neurosci Lett 410: 146–151.
7. Hodges NJ, Innocent N, Dhanda S, Graham M (2008) Cellular protection from oxidative DNA damage by over-expression of the novel globin cytoglobin in vitro. Mutagenesis 23: 293–298.
8. Nishi H, Inagi R, Kawada N, Yoshizato K, Mimura I, et al. (2011) Cytoglobin, a novel member of the globin family, protects kidney fibroblasts against oxidative stress under ischemic conditions. Am J Pathol 178: 128–139.
9. Trent JT 3rd, Hargrove MS (2002) A ubiquitously expressed human hexacoordinate hemoglobin. J Biol Chem 277: 19538–19545.
10. Schmidt M, Gerlach F, Avivi A, Laufs T, Wystub S, et al. (2004) Cytoglobin is a respiratory protein in connective tissue and neurons, which is up-regulated by hypoxia. J Biol Chem 279: 8063–8069.
11. Gorr TA, Wichmann D, Pilarsky C, Theurillat JP, Fabrizius A, et al. (2011) Old proteins-new locations: myoglobin, haemoglobin, neuroglobin and cytoglobin in solid tumours and cancer cells. Acta Physiol (Oxf) 202: 563–581.
12. Presneau N, Dewar K, Forgetta V, Provencher D, Mes-Masson AM, et al. (2005) Loss of heterozygosity and transcriptome analyses of a 1.2 Mb candidate ovarian cancer tumor suppressor locus region at 17q25.1–q25.2. Mol Carcinog 43: 141–154.
13. Xinarianos G, McRonald FE, Risk JM, Bowers NL, Nikolaidis G, et al. (2006) Frequent genetic and epigenetic abnormalities contribute to the deregulation of cytoglobin in non-small cell lung cancer. Hum Mol Genet 15: 2038–2044.
14. McRonald FE, Liloglou T, Xinarianos G, Hill L, Rowbottom L, et al. (2006) Down-regulation of the cytoglobin gene, located on 17q25, in tylosis with oesophageal cancer (TOC): evidence for trans-allele repression. Hum Mol Genet 15: 1271–1277.
15. Shaw RJ, Omar MM, Rokadiya S, Kogera FA, Lowe D, et al. (2009) Cytoglobin is upregulated by tumour hypoxia and silenced by promoter hypermethylation in head and neck cancer. Br J Cancer 101: 139–144.
16. Geuens E, Brouns I, Flamez D, Dewilde S, Timmermans JP, et al. (2003) A globin in the nucleus! J Biol Chem 278: 30417–30420.
17. Emara M, Turner AR, Allalunis-Turner J (2010) Hypoxic regulation of cytoglobin and neuroglobin expression in human normal and tumor tissues. Cancer Cell Int 10: 33.
18. Shivapurkar N, Stastny V, Okumura N, Girard L, Xie Y, et al. (2008) Cytoglobin, the newest member of the globin family, functions as a tumor suppressor gene. Cancer Res 68: 7448–7456.
19. Jones PA, Laird PW (1999) Cancer epigenetics comes of age. Nat Genet 21: 163–167.
20. Benner SE, Wahl GM, Von Hoff DD (1991) Double minute chromosomes and homogeneously staining regions in tumors taken directly from patients versus in human tumor cell lines. Anticancer Drugs 2: 11–25.
21. Wright JA, Smith HS, Watt FM, Hancock MC, Hudson DL, et al. (1990) DNA amplification is rare in normal human cells. Proc Natl Acad Sci U S A 87: 1791–1795.
22. Yasumoto K, Yokoyama K, Shibata K, Tomita Y, Shibahara S (1994) Microphthalmia-associated transcription factor as a regulator for melanocyte-specific transcription of the human tyrosinase gene. Mol Cell Biol 14: 8058–8070.
23. Yaar M, Park HY (2012) Melanocytes: a window into the nervous system. J Invest Dermatol 132: 835–845.
24. Meyskens FL Jr, Farmer P, Fruehauf JP (2001) Redox regulation in human melanocytes and melanoma. Pigment Cell Res 14: 148–154.
25. Bustamante J, Bredeston L, Malanga G, Mordoh J (1993) Role of melanin as a scavenger of active oxygen species. Pigment Cell Res 6: 348–353.
26. Gidanian S, Mentelle M, Meyskens FL Jr, Farmer PJ (2008) Melanosomal damage in normal human melanocytes induced by UVB and metal uptake–a basis for the pro-oxidant state of melanoma. Photochem Photobiol 84: 556–564.
27. Sander CS, Hamm F, Elsner P, Thiele JJ (2003) Oxidative stress in malignant melanoma and non-melanoma skin cancer. Br J Dermatol 148: 913–922.
28. Szatrowski TP, Nathan CF (1991) Production of large amounts of hydrogen peroxide by human tumor cells. Cancer Res 51: 794–798.
29. Fruehauf JP, Trapp V (2008) Reactive oxygen species: an Achilles' heel of melanoma? Expert Rev Anticancer Ther 8: 1751–1757.
30. Martindale JL, Holbrook NJ (2002) Cellular response to oxidative stress: signaling for suicide and survival. J Cell Physiol 192: 1–15.
31. Ueda Y, Richmond A (2006) NF-kappaB activation in melanoma. Pigment Cell Res 19: 112–124.
32. Gadjeva V, Dimov A, Georgieva N (2008) Influence of therapy on the antioxidant status in patients with melanoma. J Clin Pharm Ther 33: 179–185.
33. Yamaura M, Mitsushita J, Furuta S, Kiniwa Y, Ashida A, et al. (2009) NADPH oxidase 4 contributes to transformation phenotype of melanoma cells by regulating G2-M cell cycle progression. Cancer Res 69: 2647–2654.
34. Nazarewicz RR, Dikalova A, Bikineyeva A, Ivanov S, Kirilyuk IA, et al. (2013) Does scavenging of mitochondrial superoxide attenuate cancer prosurvival signaling pathways? Antioxid Redox Signal 19: 344–349.
35. Petersen MG, Dewilde S, Fago A (2008) Reactions of ferrous neuroglobin and cytoglobin with nitrite under anaerobic conditions. J Inorg Biochem 102: 1777–1782.
36. Fujita Y, Islam R, Sakai K, Kaneda H, Kudo K, et al. (2012) Aza-derivatives of resveratrol are potent macrophage migration inhibitory factor inhibitors. Invest New Drugs 30: 1878–1886.
37. Kudo K, Arao T, Tanaka K, Nagai T, Furuta K, et al. (2011) Antitumor activity of BIBF 1120, a triple angiokinase inhibitor, and use of VEGFR2+pTyr+ peripheral blood leukocytes as a pharmacodynamic biomarker in vivo. Clin Cancer Res 17: 1373–1381.
38. Kaneda H, Arao T, Tanaka K, Tamura D, Aomatsu K, et al. (2010) FOXQ1 is overexpressed in colorectal cancer and enhances tumorigenicity and tumor growth. Cancer Res 70: 2053–2063.
39. Kaneda H, Arao T, Matsumoto K, De Velasco MA, Tamura D, et al. (2011) Activin A inhibits vascular endothelial cell growth and suppresses tumour angiogenesis in gastric cancer. Br J Cancer 105: 1210–1217.

Biomarkers of reactive resistance and early disease progression during chemotherapy plus bevacizumab treatment for colorectal carcinoma

Hidetoshi Hayashi[1,2,3], Tokuzo Arao[1], Kazuko Matsumoto[1], Hideharu Kimura[1], Yosuke Togashi[1], Yoshinori Hirashima[4,5], Yosuke Horita[4,6], Satoru Iwasa[4], Natsuko Tsuda Okita[4], Yoshitaka Honma[4], Atsuo Takashima[4], Ken Kato[4], Tetsuya Hamaguchi[4], Yasuhiro Shimada[4], Kazuhiko Nakagawa[2], Kazuto Nishio[1], and Yasuhide Yamada[4]

[1] Department of Genome Biology, Kinki University Faculty of Medicine, Osakasayama City, Osaka, Japan.

[2] Department of Medical Oncology, Kinki University Faculty of Medicine, Osakasayama City, Osaka, Japan.

[3] Department of Medical Oncology, Kishiwada Municipal Hospital, Kishiwada, Osaka, Japan.

[4] Gastrointestinal Medical Oncology Division, National Cancer Center Hospital, Chuo-ku, Tokyo, Japan.

[5] Department of Medical Oncology, Oita University, Hazama-cho, Yufu, Oita, Japan.

[6] Department of Chemotherapy, Toyama Prefectural Central Hospital, Toyama, Toyama, Japan.

Correspondence to: *Hidetoshi Hayashi,* ***email:*** *hidet31@gmail.com*

Keywords: placental growth factor (PlGF), vascular endothelial growth factor (VEGF), colorectal carcinoma, bevacizumab, angiogenesis

Received: *January 5, 2014* ***Accepted:*** *March 20, 2014* ***Published:*** *March 22, 2014*

ABSTRACT:

Molecular markers for predicting or monitoring the efficacy of bevacizumab in patients with metastatic colorectal cancer (mCRC) remain to be identified. We have now measured the serum concentrations of 25 angiogenesis-related molecules with antibody suspension bead array systems for 25 mCRC patients both before and during treatment in a previously reported phase II trial of FOLFIRI chemotherapy plus bevacizumab. The serum concentration of vascular endothelial growth factor–A (VEGF-A) decreased after the onset of treatment ($P < 0.0001$), whereas that of placental growth factor increased ($P < 0.0001$). Significant differences in the levels of several factors (such as VEGF-A, soluble VEGF receptor–2, and interleukin-8) were apparent between responders and nonresponders during treatment. The rapid and pronounced decrease in serum VEGF-A level after treatment onset was apparent in all subjects and was independent of the baseline concentration. However, four of nine nonresponders showed a subsequent early increase in the serum VEGF-A level. Our results thus suggest that an early increase in the serum VEGF-A concentration after the initial decrease is a potential predictive marker of a poor response and reactive resistance to bevacizumab plus chemotherapy.

INTRODUCTION

Angiogenesis, defined as the formation of new blood vessels from a preexisting vasculature, is essential for tumor growth and the spread of metastases [1, 2]. Inhibition of angiogenesis is therefore considered a promising strategy for cancer treatment, with clinical application of this strategy being pursued in the form of multiple modalities that include the development of specific inhibitors of signaling by vascular endothelial growth factor (VEGF) and its cognate receptors (VEGFRs). Bevacizumab is a humanized monoclonal antibody specific for VEGF-A, a key inducer of angiogenesis in tumors, and it has been found to manifest

clinical activity in patients with metastatic colorectal cancer (mCRC) [3]. Furthermore, the cytotoxicity of chemotherapy is blunted by the production of VEGF and other proangiogenic factors that recruit new endothelial cells and protect them from chemotherapy, and bevacizumab transiently "normalizes" the abnormal structure and function of the tumor vasculature to render it more efficient for oxygen and drug delivery [4]. Indeed, bevacizumab is effective against metastatic colorectal cancer (mCRC) mainly in combination with chemotherapeutic drugs.

The efficacy of chemotherapy plus bevacizumab varies among patients, however, and so the ability to identify tumors likely to be most sensitive to such treatment would help to optimize the implementation of this approach as well as provide important insight into the mechanisms of resistance. The identification of a biomarker predictive of bevacizumab treatment outcome has proven to be challenging. Angiogenesis is a complex and highly adaptive biological process, with multiple factors in addition to VEGF-A playing an essential role, including placental growth factor (PlGF), fibroblast growth factors (FGFs), platelet-derived growth factor (PDGF), angiopoietins, and various additional cytokines [5]. Reactive resistance to bevacizumab in combination with chemotherapy is mediated in part by hypoxia-inducible factor–1 (HIF-1) and its transcriptional activation of genes for multiple factors including VEGF-A and FGFs.

Extensive biomarker analysis has been conducted in numerous clinical trials of bevacizumab, with evaluation of the relation between circulating VEGF-A levels at baseline and treatment outcome having been performed in most cases [6]. Although a few studies have detected a significant correlation between the baseline serum concentration of VEGF-A and the outcome of antiangiogenic therapy [7], many others have not. The inconsistency of these results emphasizes the need for evaluation of predictive biomarkers in a dynamic manner—that is, before and after the onset of antiangiogenic treatment.

We have previously described a phase II study (AVASIRI trial) designed to investigate the efficacy of a bevacizumab plus FOLFIRI (folinic acid, 5-fluorouracil, irinotecan) regimen as a second-line treatment for individuals with metastatic colorectal cancer (mCRC) [8]. Promising results were obtained with regard to response rate (32%), progression-free survival (PFS) time (median of 11.6 months), and overall survival (OS) time (median of 21.4 months). Serum samples were collected at various time points during the trial for measurement of the levels of 25 angiogenesis-related molecules. We now present the results of the analysis of these serum samples from the AVASIRI trial.

RESULTS

Patient characteristics

Serum samples were available for all 25 patients treated with FOLFIRI and bevacizumab. The characteristics of the study patients are shown in Table 1. The median age was 62 years (range, 38–73), and the male/female distribution was 20/5. The overall response rate was 32%, with 8 patients showing a partial response, 15 stable disease, and 2 disease progression. Median progression-free survival (PFS) and overall survival (OS) were 11.6 months [95% confidence interval (CI), 6.9–16.4] and 21.4 months (95% CI, 12.0–30.8), respectively.

Circulating levels of angiogenesis-related molecules before and during treatment with FOLFIRI and bevacizumab

We examined changes in the serum concentrations of 25 angiogenesis-related molecules between before (baseline) and after the onset of treatment with FOLFIRI plus bevacizumab (Figure 1). The baseline serum concentrations varied widely among individuals, with the values for VEGF-A, for example, ranging from 13 to 907 pg/mL. Significant changes in the serum levels of various molecules were apparent at various time points during treatment compared with baseline (Figure 2). Of note, the serum concentration of VEGF-A decreased markedly after the onset of treatment (from 337.7 ± 244.4 pg/mL at baseline to 1.9 ± 5.0, 5.6 ± 12.6, 8.2 ± 17.5, and 7.3 ± 20.8 pg/mL at 1, 2, 4, and 6 months, respectively; $P < 0.0001$), whereas that of PlGF showed a pronounced increase (from 4.1 ± 3.4 pg/mL at baseline to 17.6 ± 9.0, 19.9 ± 7.9, 21.9 ± 12.3, and 24.4 ± 10.8 pg/mL at 1, 2, 4, and 6 months, respectively; $P < 0.0001$). Given that these results were obtained with paired samples from the same individuals at baseline and after the onset of treatment, the observed changes were likely attributable to the administration of FOLFIRI plus bevacizumab.

Serum concentrations of angiogenesis-related molecules and PFS

We divided the patients into two groups on the basis of progression-free survival (PFS) time. Given that the median PFS for patients with mCRC treated with chemotherapy plus bevacizumab in the second-line setting was previously found to be ~7 months [9], we dichotomized our patient population according to a PFS of 7 months (responders, ≥7 months; nonresponders, <7 months). None of the 25 molecules examined served as a predictive marker on the basis of the baseline serum

Table 1: Summary of patient characteristics and AVASIRI trial results.

Median (range) age of patients (years)	62 (38–73)
ECOG performance status 0/1	16/9
Male/female	20/5
Primary lesion in colon/rectum	12/13
Prior treatment with/without FOLFOX	16/9
Overall response rate (%)	32 (90% CI, 17.0–50.4)
Median PFS (days)	349 (95% CI, 207–491)
Median OS (days)	642 (95% CI, 359–925)

Abbreviations not defined in text: ECOG, Eastern Cooperative Oncology Group; FOLFOX, folinic acid plus 5-fluorouracil plus oxaliplatin.

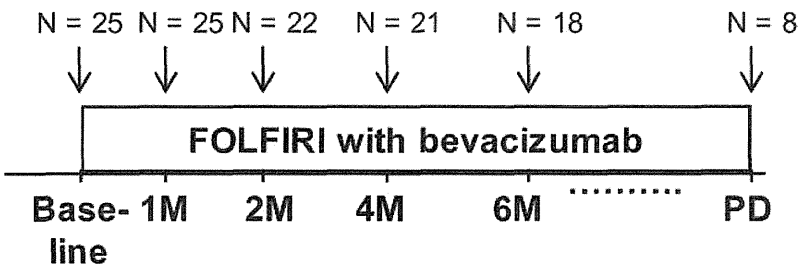

Figure 1: Flow diagram for analysis of the study subjects. Paired serum samples were available for 25 patients at baseline and at 1 month after the onset of treatment, for 22 patients at 2 months, for 21 patients at 4 months, for 18 patients at 6 months, and for 8 patients at the onset of progressive disease (PD) or last follow-up.

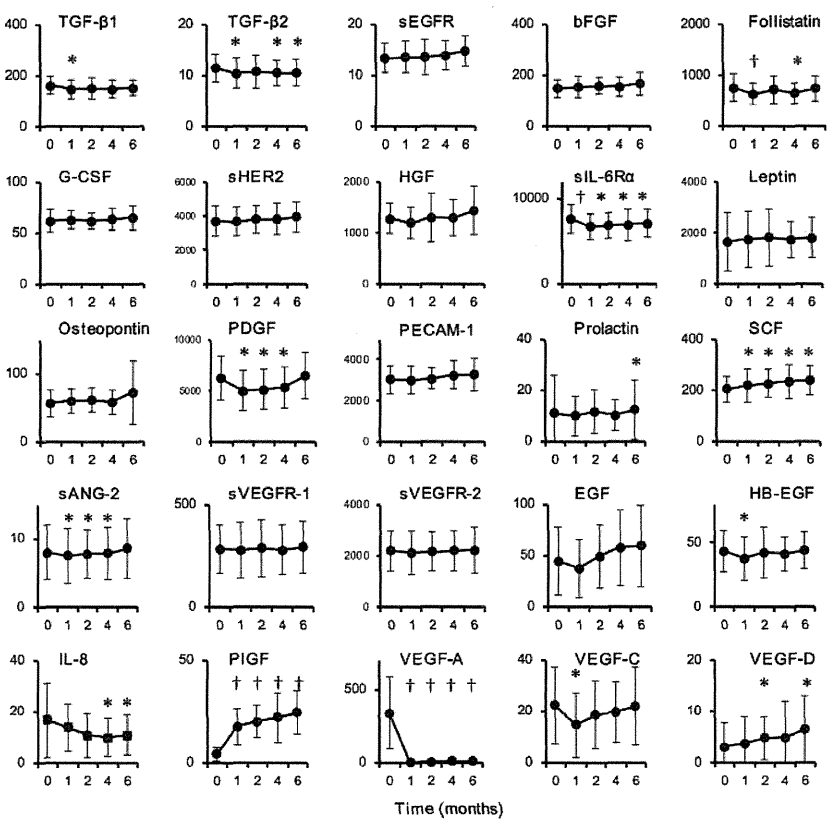

Figure 2: Serum concentrations of 25 angiogenesis-related molecules at baseline and at 1, 2, 4, and 6 months after the onset of FOLFIRI with bevacizumab treatment. Data are means ± SD for the numbers of samples indicated in Figure 1. *$P < 0.05$, †$P < 0.0001$ versus the corresponding baseline value (Student's paired t test). All values represent picograms per milliliter.

concentrations, whereas significant differences in the levels of various molecules [including soluble VEGFR-2 (sVEGFR-2), interleukin (IL)–8, VEGF-A, and VEGF-C] at various time points during treatment were apparent between responders and nonresponders (Table 2).

Relation between FOLFIRI-bevacizumab treatment and changes in serum VEGF-A level

Finally, we investigated the relation between changes in the serum concentration of VEGF-A and the duration of treatment with FOLFIRI plus bevacizumab (Figure 3). Several patients manifested an increase in the serum VEGF-A level around the time of disease progression relative to the lowered value apparent after the onset of treatment and during its administration for several months. Of note, four nonresponders showed an early increase in the serum concentration of VEGF-A (cases 17–20 in Figure 3B). The PFS of these four patients was significantly shorter than that of the other 21 patients (200 versus 373 days, respectively; $P = 0.009$, Student's unpaired t test), suggesting that an early increase in serum VEGF-A level subsequent to an initial decrease is predictive of early resistance to bevacizumab. On the other hand, the serum concentration of VEGF-A remained stable at the time of disease progression in other patients (cases 13–16). Patient 15 continued treatment with bevacizumab, in combination with a different chemotherapy regimen (mFOLFOX6), beyond disease progression.

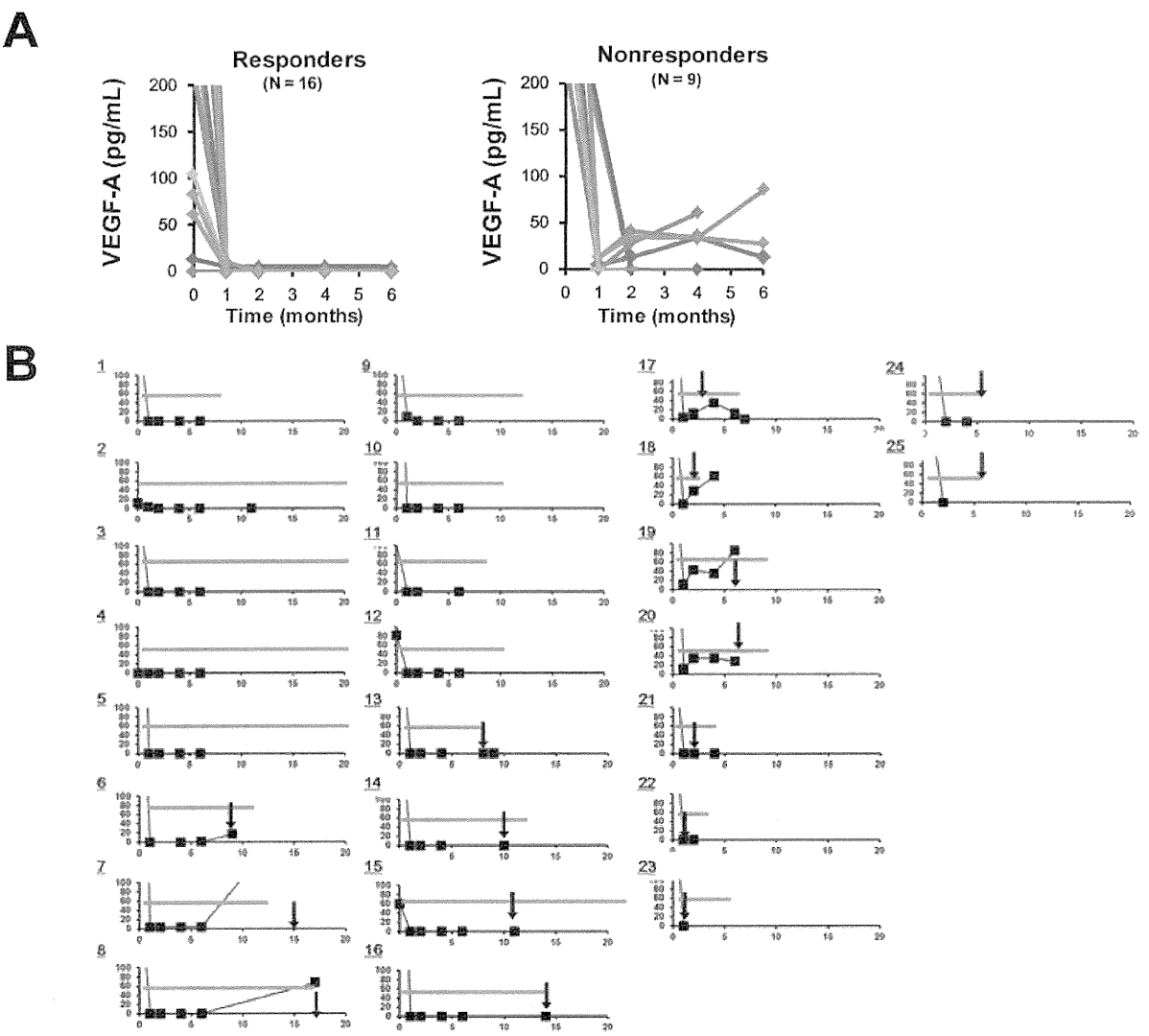

Figure 3: Analysis of changes in the serum concentration of VEGF-A. (A) Time course of serum VEGF-A level in responders and nonresponders. (B) Time course of serum VEGF-A concentration in relation to the duration of treatment with bevacizumab plus chemotherapy (gray bars) and the detection of disease progression (black arrows). Cases 1 to 16 and 17 to 25 correspond to responders and nonresponders, respectively. The vertical and horizontal axes represent serum VEGF-A (pg/mL) and time (months), respectively.

Table 2: Serum concentrations of 25 angiogenesis-related molecules at baseline and at the indicated times after the onset of treatment with FOLFIRI plus bevacizumab in responders and nonresponders. Data are means ± SD. The P values for comparisons between responders (RES) and nonresponders (non-RES) were determined with Student's unpaired t test; those of <0.05 are shown in bold.

	Serum concentration (pg/ml)														
	Baseline (N = 25)			1 month (N = 25)			2 months (N = 22)			4 months (N = 21)			6 months (N = 18)		
	RES	non-RES	*P* value	RES	non-RES	*P* value	RES	non-RES	*P* value	RES	non-RES	*P* value	RES	non-RES	*P* value
TGF-β1	164 ± 33	149 ± 46	0.443	145 ± 39	138 ± 46	0.732	142 ± 32	159 ± 70	0.594	151 ± 35	121 ± 26	0.067	157 ± 29	123 ± 28	0.086
TGF-β2	12 ± 3	12 ± 3	0.818	10 ± 3	10 ± 3	0.961	11 ± 4	12 ± 2	0.379	11 ± 3	10 ± 1	0.362	11 ± 3	9 ± 1	0.176
sEGFR	13 ±3	14 ± 4	0.838	13 ± 3	14 ± 4	0.571	13 ± 3	15 ± 4	0.241	13 ± 3	16 ± 3	0.190	14 ± 3	18 ± 2	**0.018**
bFGF	146 ± 38	159 ± 26	0.352	150 ± 47	167 ± 33	0.346	149 ± 35	182 ± 25	**0.031**	149 ± 40	177 ± 29	0.115	157 ± 43	195 ± 39	0.156
Follistatin	736 ± 310	766 ± 198	0.783	627 ± 257	603 ± 143	0.778	664 ± 206	860 ± v388	0.284	620 ± 202	745 ± 185	0.242	655 ± 227	997 ± 131	**0.004**
G-CSF	61 ± 11	64 ± 10	0.610	63 ± 10	62 ± 8	0.947	62 ± 7	60 ± 11	0.719	65 ± 10	59 ± 12	0.347	64 ± 10	65 ± 19	0.966
sHER2	3697 ± 920	3914 ± 811	0.580	3645 ± 971	3906 ± 599	0.443	3615 ± 917	4207 ± 306	**0.040**	3737 ± 840	4148 ± 1011	0.443	3700 ± 856	4686 ± 429	**0.010**
HGF	1222 ± 279	1470 ± 303	0.093	1155 ± 325	1332 ± 289	0.216	1157 ± 293	1660 ± 674	0.131	1201 ± 274	1599 ± 422	0.103	1289 ± 362	1921 ± 573	0.110
sIL-6Rα	7883 ± 1714	6899 ± 1465	0.183	7037 ± 1562	5905 ± 825	**0.035**	6981 ± 1672	6097 ± 700	0.104	7020 ± 1616	6266 ± 2505	0.555	7134 ± 1715	6816 ± 1467	0.727
Leptin	1608 ± 1048	2038 ± 1364	0.475	1704 ± 1045	2119 ± 1237	0.457	1765 ± 912	2054 ± 1592	0.690	1823 ± 702	1625 ± 805	0.640	1903 ± 836	1379 ± 455	0.133
Osteopontin	54 ± 21	59 ± 18	0.582	58 ± 20	61 ± 16	0.665	57 ± 17	67 ± 21	0.366	54 ± 12	67 ± 32	0.441	65 ± 31	95 ± 86	0.538
PDGF	6297 ± 2439	6488 ± 1321	0.812	4978 ± 2276	5095 ± 1460	0.884	4770 ± 2124	5874 ± 1753	0.246	5224 ± 2244	5372 ± 1825	0.885	6095 ± 2085	7582 ± 2702	0.365
PECAM-1	3034 ± 749	3116 ± 469	0.753	3018 ± 746	3081 ± 548	0.823	2959 ± 544	3294 ± 257	0.072	3211 ± 785	3468 ± 323	0.317	3097 ± 760	3857 ± 711	0.121
Prolactin	10 ± 17	10 ± 5	0.964	9 ± 9	11 ± 5	0.451	11 ± 9	15 ± 9	0.374	10 ± 6	13 ± 8	0.450	8 ± 4	26 ± 19	0.159
SCF	207 ± 55	210 ± 44	0.892	218 ± 62	235 ± 71	0.587	218 ± 55	249 ± 55	0.270	226 ± 55	276 ± 91	0.297	227 ± 61	279 ± 20	**0.016**
sANG-2	8 ± 4	10 ± 3	0.139	7 ± 4	9 ± 3	0.292	7 ± 4	10 ± 2	**0.030**	7 ± 4	11 ± 3	**0.027**	8 ± 4	12 ± 3	0.062
sVEGFR-1	289 ± 139	289 ± 67	0.997	282 ± 166	268 ± 67	0.774	261 ± 133	358 ± 148	0.199	264 ± 123	324 ± 120	0.366	275 ± 140	344 ± 68	0.201
sVEGFR-2	2128 ± 873	2388 ± 662	0.445	2067 ± 917	2338 ± 785	0.483	2001 ± 750	2567 ± 799	0.171	1995 ± 792	2794 ± 418	**0.012**	2004 ± 887	2936 ± 473	**0.020**
EGF	50 ± 34	26 ± 28	0.097	38 ± 30	31 ± 28	0.628	58 ± 32	31 ± 21	**0.038**	59 ± 39	56 ± 37	0.861	59 ± 40	62 ± 43	0.882
HB-EGF	44 ± 14	42 ± 24	0.897	39 ± 13	38 ± 26	0.966	40 ± 13	48 ± 32	0.573	43 ± 14	35 ± 9	0.138	46 ± 15	35 ± 12	0.183
IL-8	14 ± 15	24 ± 13	0.115	10 ± 6	19 ± 7	**0.027**	8 ± 6	17 ± 11	0.109	8 ± 6	15 ± 10	0.216	9 ± 6	18 ± 10	0.165
PlGF	4 ± 3	5 ± 4	0.635	17 ± 9	20 ± 9	0.473	19 ± 8	19 ± 6	0.878	18 ± 7	34 ± 18	0.127	22 ± 8	33 ± 15	0.246
VEGF-A	333 ± 295	351 ± 143	0.842	1 ± 3	4 ± 6	0.228	0 ± 1	20 ± 18	**0.046**	0 ± 1	33 ± 22	**0.027**	0 ± 1	42 ± 38	0.198
VEGF-C	23 ± 16	23 ± 16	0.995	15 ± 15	16 ± 7	0.813	16 ± 13	27 ± 12	0.082	17 ± 12	28 ± 8	**0.047**	21 ± 16	25 ± 11	0.603
VEGF-D	3 ± 3	1 ± 2	0.235	4 ± 4	1 ± 2	0.083	5 ± 4	4 ± 6	0.626	5 ± 8	6 ± 5	0.713	6 ± 6	7 ± 8	0.765

DISCUSSION

The introduction of novel molecularly targeted therapies, including antiangiogenic and anti–epidermal growth factor receptor (EGFR) agents, has increased the options available for treatment of mCRC [9]. At present, bevacizumab in combination with fluoropyrimidine-based chemotherapy is widely recognized as a standard treatment for mCRC [3, 9, 10]. However, no biomarker has previously been identified as a predictor of benefit from bevacizumab treatment, with the identification of such a molecular biomarker being a current priority of clinical research [11]. In the present study, we have addressed this issue by measuring the serum levels of multiple angiogenesis-related factors both before and during treatment of mCRC patients with bevacizumab plus FOLFIRI.

Most previous studies have found that the circulating concentration of VEGF-A, as measured with standard enzyme-linked immunosorbent assays, increases after the onset of antiangiogenic treatment [7, 12-18], whereas more recent studies have shown a decrease in VEGF-A levels after treatment onset [19-21]. We have now shown that treatment with bevacizumab plus chemotherapy was associated with a rapid and highly significant decrease in the serum concentration of VEGF-A that was independent of the baseline concentration and which, in most cases, remained apparent throughout the duration of therapy, similar to the results of a previous pharmacodynamic analysis of angiogenesis-related factors [22]. Although it remains unclear whether circulating VEGF-A in individuals treated with bevacizumab is free or bound to the antibody, given that bevacizumab is administered at doses high enough to give rise to such binding, our results suggest that the antibody suspension bead array system adopted in the present study measures VEGF-A that is free of bevacizumab.

An initial decrease in serum VEGF-A level was observed in all patients of the present study. However, some patients manifested a subsequent early small but definite increase in this parameter. This latter finding may be related to the assay measuring free VEGF-A and may therefore reflect a compensatory increase in the circulating concentration of this factor. Our observation that the PFS of such patients was shorter than that of the other subjects suggests that the development of acquired resistance to bevacizumab treatment may be driven in part by loss of the ability to suppress the circulating level of free VEGF-A. VEGF-A promotes the survival of and increases resistance to chemotherapy in cancer cells. Chemotherapy acts as an "accidental" antiangiogenic therapy (action), whereas VEGF-A and other proangiogenic factors recruit new endothelial cells and protect them from the cytotoxicity of chemotherapy (reaction) [4, 23]. Bevacizumab is thought to block this reaction. From this perspective, our results suggest that an early increase in VEGF-A levels after the initial decrease is a potential predictive marker of reactive resistance to bevacizumab that results in a shorter PFS in patients treated with the combination of FOLFIRI and bevacizumab.

Despite the predominant role of VEGF-A, multiple other factors contribute to regulation of the complex and highly adaptive process of angiogenesis. Investigation of potential biomarkers other than VEGF-A is thus important, given the role of these other factors in tumor angiogenesis and vessel maturation. However, only a few studies have previously examined multiple angiogenesis-related proteins during bevacizumab treatment in a dynamic

manner [22]. We have now detected significant treatment-induced changes in the serum concentrations of several angiogenesis-related molecules including PlGF. Previous biomarker analyses also described an increase in the circulating concentration of PlGF in response to VEGF-targeted treatment [12, 14, 15, 17, 22]. Indeed, targeting of PlGF is under consideration as a novel approach to prevent tumor escape from VEGF-targeted therapy [24]. However, we did not detect a significant difference in serum PlGF levels after bevacizumab administration between responders and nonresponders in the present study. A previous study also found that the combination of antibodies to PlGF and those to VEGF-A did not yield a greater antitumor effect in vitro or in vivo compared with antibodies to VEGF-A alone [25]. Our data thus suggest that the increase in circulating PlGF level observed after the onset of bevacizumab treatment does not play a major role in the development of resistance to bevacizumab in the clinical setting.

On the other hand, we detected significantly higher serum concentrations of several angiogenesis-related factors [such as IL-8, soluble angiopoietin II (sANG-2), basic FGF (bFGF), stem cell factor (SCF), and VEGF-C] in nonresponders compared with responders at various time points during treatment. Resistance to VEGF-A pathway inhibitors might occur through VEGF-A–independent mechanisms, such as up-regulation of other proangiogenic factors [26-28]. Given that targeting of these molecules may provide a basis for novel approaches to prevent tumor escape from bevacizumab treatment, further analysis of multiple angiogenesis-related factors in a large number of patients is warranted.

In conclusion, our present results indicate that an early increase in the serum concentration of VEGF-A after the initial decrease may be a potential predictive marker of a poor response and reactive resistance to bevacizumab plus chemotherapy.

METHODS

Patients

The main inclusion criteria for the present study were the same as those previously described for the AVASIRI trial [8]. In brief, they comprised a histologically confirmed diagnosis of colorectal cancer; failure of first-line treatment with 5-fluorouracil– or oxaliplatin-based chemotherapy without bevacizumab or CPT-11 (irinotecan); measurable disease according to RECIST (ver. 1.0); and metastatic disease deemed unresectable at baseline. Enrolled patients received biweekly administrations of the FOLFIRI regimen, consisting of CPT-11 (150 mg/m^2) on day 1, given as a 2-h infusion concurrent with leucovorin (folinic acid, 200 mg/m^2), followed by 5-fluorouracil given by injection (400 mg/m^2) and then as a 46-h continuous infusion (2400 mg/m^2). Bevacizumab was administered at a biweekly dose of 10 mg/kg before the FOLFIRI regimen. Treatment was discontinued in the event of disease progression, unacceptable toxicity, or withdrawal of consent. Patients underwent a computed tomography scan after every four cycles of treatment for evaluation of tumor response. They provided written informed consent to receive the treatment and to participate in translational analyses.

Sample collection and analysis

Blood samples were obtained from all assigned patients at baseline (before the first dose of study drugs) as well as at 1, 2, 4, and 6 months after the onset of the treatment protocol (Figure 1). In addition, blood samples from eight patients who received the study treatment for >6 months were obtained at the time of disease progression or last follow-up. Serum separated from the blood samples was stored at –80°C until analysis.

The serum levels of VEGF-A, VEGF-C, VEGF-D, PlGF, epidermal growth factor (EGF), IL-8, and heparin-binding EGF-like growth factor (HB-EGF) were measured with the use of a Milliplex MAP Human Angiogenesis/Growth Factor Magnetic Bead Panel (Merck Millipore, Billerica, MA, USA). Magnetic antibody-conjugated beads were subjected to ultrasonic treatment for 30 s and then to vortex-mixing for 1 min in order to reduce bead aggregation. All samples, quality controls, and standards were prepared as recommended with the supplied diluents and were processed in duplicate batches. Assay buffer (200 μL) was added to each well and then decanted. Each sample (25 μL) and the prepared beads (25 μL) were then added to the wells together with buffering solutions. The plate was sealed, incubated overnight at 4°C, and washed three times, after which detection antibodies (25 μL) were added to each well and the plate was incubated for 1 h at room temperature. Streptavidin-phycoerythrin (25 μL) was then added to each well, after which the plate was incubated for an additional 30 min at room temperature and washed three times. Sheath fluid (100 μL) was finally added to each well, and the assay plate was analyzed with the Luminex 100 instrument.

The serum levels of transforming growth factor (TGF)–β1 and TGF-β2 were measured with a Milliplex MAP Multi-Species TGFβ 3-Plex panel (Merck Millipore), whereas those of various additional factors related to angiogenesis were measured with a Bio-Plex Pro Human Cancer Biomarker Panel 1, 16-Plex (Bio-Rad, Hercules, CA, USA) as previously described [29]. The latter factors included soluble EGFR (sEGFR), bFGF, osteopontin, PDGF–AB/BB, follistatin, granulocyte colony-stimulating factor (G-CSF), platelet endothelial cell adhesion molecule–1 (PECAM-1), prolactin, soluble human EGF receptor 2/NEU (sHER2/NEU), hepatocyte

growth factor (HGF), SCF, sANG-2, soluble IL-6 receptor α (sIL-6Rα), leptin, sVEGFR-1, and sVEGFR-2.

Statistical analysis

Serum factor levels at baseline (pretreatment) were compared with those at 1, 2, 4, or 6 months after treatment onset with the use of Student's paired *t* test in order to evaluate the significance of changes induced by the study treatment. The relations between treatment efficacy and serum factor levels were analyzed with Student's unpaired *t* test. A *P* value of <0.05 was considered statistically significant. All statistical tests were performed with SPSS version 14.0 software (SPSS, Chicago, IL, USA).

ACKNOWLEDGMENTS

We thank Shinji Kurashimo, Yoshihiro Mine, Ayaka Kurumatani, and Tomoko Kitayama for technical assistance. This study was supported by The Third-Term Comprehensive 10-Year Strategy for Cancer Control of, and by a Grant-in-Aid for Cancer Research from, the Ministry of Health, Labor, and Welfare of Japan. The authors declare no conflicts of interest.

REFERENCES

1. Taylor M, Rossler J, Geoerger B, Laplanche A, Hartmann O, Vassal G, Farace F. High levels of circulating VEGFR2+ Bone marrow-derived progenitor cells correlate with metastatic disease in patients with pediatric solid malignancies. Clin Cancer Res 2009; 15: 4561-4571.
2. Kerbel R, Folkman J. Clinical translation of angiogenesis inhibitors. Nat Rev Cancer 2002; 2: 727-739.
3. Hurwitz H, Fehrenbacher L, Novotny W, Cartwright T, Hainsworth J, Heim W, Berlin J, Baron A, Griffing S, Holmgren E, Ferrara N, Fyfe G, Rogers B, Ross R, Kabbinavar F. Bevacizumab plus irinotecan, fluorouracil, and leucovorin for metastatic colorectal cancer. N Engl J Med 2004; 350: 2335-2342.
4. Blagosklonny MV. How Avastin potentiates chemotherapeutic drugs: action and reaction in antiangiogenic therapy. Cancer Biol Ther 2005; 4: 1307-1310.
5. Carmeliet P, Jain RK. Molecular mechanisms and clinical applications of angiogenesis. Nature 2011; 473: 298-307.
6. Lambrechts D, Lenz HJ, de Haas S, Carmeliet P, Scherer SJ. Markers of response for the antiangiogenic agent bevacizumab. J Clin Oncol 2013; 31: 1219-1230.
7. Burstein HJ, Chen YH, Parker LM, Savoie J, Younger J, Kuter I, Ryan PD, Garber JE, Chen H, Campos SM, Shulman LN, Harris LN, Gelman R, Winer EP. VEGF as a marker for outcome among advanced breast cancer patients receiving anti-VEGF therapy with bevacizumab and vinorelbine chemotherapy. Clin Cancer Res 2008; 14: 7871-7877.
8. Horita Y, Yamada Y, Kato K, Hirashima Y, Akiyoshi K, Nagashima K, Nakajima T, Hamaguchi T, Shimada Y. Phase II clinical trial of second-line FOLFIRI plus bevacizumab for patients with metastatic colorectal cancer: AVASIRI trial. Int J Clin Oncol 2012; 17: 604-609.
9. Giantonio BJ, Catalano PJ, Meropol NJ, O'Dwyer PJ, Mitchell EP, Alberts SR, Schwartz MA, Benson AB, 3rd. Bevacizumab in combination with oxaliplatin, fluorouracil, and leucovorin (FOLFOX4) for previously treated metastatic colorectal cancer: results from the Eastern Cooperative Oncology Group Study E3200. J Clin Oncol 2007; 25: 1539-1544.
10. Cassidy J, Clarke S, Diaz-Rubio E, Scheithauer W, Figer A, Wong R, Koski S, Lichinitser M, Yang TS, Rivera F, Couture F, Sirzen F, Saltz L. Randomized phase III study of capecitabine plus oxaliplatin compared with fluorouracil/folinic acid plus oxaliplatin as first-line therapy for metastatic colorectal cancer. J Clin Oncol 2008; 26: 2006-2012.
11. Shaked Y, Bocci G, Munoz R, Man S, Ebos JM, Hicklin DJ, Bertolini F, D'Amato R, Kerbel RS. Cellular and molecular surrogate markers to monitor targeted and non-targeted antiangiogenic drug activity and determine optimal biologic dose. Curr Cancer Drug Targets 2005; 5: 551-559.
12. Batchelor TT, Sorensen AG, di Tomaso E, Zhang WT, Duda DG, Cohen KS, Kozak KR, Cahill DP, Chen PJ, Zhu M, Ancukiewicz M, Mrugala MM, Plotkin S, Drappatz J, Louis DN, Ivy P, Scadden DT, Benner T, Loeffler JS, Wen PY, Jain RK. AZD2171, a pan-VEGF receptor tyrosine kinase inhibitor, normalizes tumor vasculature and alleviates edema in glioblastoma patients. Cancer Cell 2007; 11: 83-95.
13. Norden-Zfoni A, Desai J, Manola J, Beaudry P, Force J, Maki R, Folkman J, Bello C, Baum C, DePrimo SE, Shalinsky DR, Demetri GD, Heymach JV. Blood-based biomarkers of SU11248 activity and clinical outcome in patients with metastatic imatinib-resistant gastrointestinal stromal tumor. Clin Cancer Res 2007; 13: 2643-2650.
14. Zhu AX, Sahani DV, Duda DG, di Tomaso E, Ancukiewicz M, Catalano OA, Sindhwani V, Blaszkowsky LS, Yoon SS, Lahdenranta J, Bhargava P, Meyerhardt J, Clark JW, Kwak EL, Hezel AF, Miksad R, Abrams TA, Enzinger PC, Fuchs CS, Ryan DP, Jain RK. Efficacy, safety, and potential biomarkers of sunitinib monotherapy in advanced hepatocellular carcinoma: a phase II study. J Clin Oncol 2009; 27: 3027-3035.
15. Willett CG, Duda DG, di Tomaso E, Boucher Y, Ancukiewicz M, Sahani DV, Lahdenranta J, Chung DC, Fischman AJ, Lauwers GY, Shellito P, Czito BG, Wong TZ, Paulson E, Poleski M, Vujaskovic Z, Bentley R, Chen HX, Clark JW, Jain RK. Efficacy, safety, and biomarkers of neoadjuvant bevacizumab, radiation therapy, and fluorouracil in rectal cancer: a multidisciplinary phase II

study. J Clin Oncol 2009; 27: 3020-3026.

16. Willett CG, Boucher Y, Duda DG, di Tomaso E, Munn LL, Tong RT, Kozin SV, Petit L, Jain RK, Chung DC, Sahani DV, Kalva SP, Cohen KS, Scadden DT, Fischman AJ, Clark JW, Ryan DP, Zhu AX, Blaszkowsky LS, Shellito PC, Mino-Kenudson M, Lauwers GY. Surrogate markers for antiangiogenic therapy and dose-limiting toxicities for bevacizumab with radiation and chemotherapy: continued experience of a phase I trial in rectal cancer patients. J Clin Oncol 2005; 23: 8136-8139.
17. Rini BI, Michaelson MD, Rosenberg JE, Bukowski RM, Sosman JA, Stadler WM, Hutson TE, Margolin K, Harmon CS, DePrimo SE, Kim ST, Chen I, George DJ. Antitumor activity and biomarker analysis of sunitinib in patients with bevacizumab-refractory metastatic renal cell carcinoma. J Clin Oncol 2008; 26: 3743-3748.
18. Saltz LB, Rosen LS, Marshall JL, Belt RJ, Hurwitz HI, Eckhardt SG, Bergsland EK, Haller DG, Lockhart AC, Rocha Lima CM, Huang X, DePrimo SE, Chow-Maneval E, Chao RC, Lenz HJ. Phase II trial of sunitinib in patients with metastatic colorectal cancer after failure of standard therapy. J Clin Oncol 2007; 25: 4793-4799.
19. Del Vecchio M, Mortarini R, Canova S, Di Guardo L, Pimpinelli N, Sertoli MR, Bedognetti D, Queirolo P, Morosini P, Perrone T, Bajetta E, Anichini A. Bevacizumab plus fotemustine as first-line treatment in metastatic melanoma patients: clinical activity and modulation of angiogenesis and lymphangiogenesis factors. Clin Cancer Res 2010; 16: 5862-5872.
20. Pectasides D, Papaxoinis G, Kalogeras KT, Eleftheraki AG, Xanthakis I, Makatsoris T, Samantas E, Varthalitis I, Papakostas P, Nikitas N, Papandreou CN, Pentheroudakis G, Timotheadou E, Koutras A, Sgouros J, Bafaloukos D, Klouvas G, Economopoulos T, Syrigos KN, Fountzilas G. XELIRI-bevacizumab versus FOLFIRI-bevacizumab as first-line treatment in patients with metastatic colorectal cancer: a Hellenic Cooperative Oncology Group phase III trial with collateral biomarker analysis. BMC Cancer 2012; 12: 271.
21. Karihtala P, Maenpaa J, Turpeenniemi-Hujanen T, Puistola U. Front-line bevacizumab in serous epithelial ovarian cancer: biomarker analysis of the FINAVAST trial. Anticancer Res 2010; 30: 1001-1006.
22. Loupakis F, Cremolini C, Fioravanti A, Orlandi P, Salvatore L, Masi G, Di Desidero T, Canu B, Schirripa M, Frumento P, Di Paolo A, Danesi R, Falcone A, Bocci G. Pharmacodynamic and pharmacogenetic angiogenesis-related markers of first-line FOLFOXIRI plus bevacizumab schedule in metastatic colorectal cancer. Br J Cancer 2011; 104: 1262-1269.
23. Blagosklonny MV. Antiangiogenic therapy and tumor progression. Cancer Cell 2004; 5: 13-17.
24. Fischer C, Jonckx B, Mazzone M, Zacchigna S, Loges S, Pattarini L, Chorianopoulos E, Liesenborghs L, Koch M, De Mol M, Autiero M, Wyns S, Plaisance S, Moons L, van Rooijen N, Giacca M, Stassen JM, Dewerchin M, Collen D, Carmeliet P. Anti-PlGF inhibits growth of VEGF(R)-inhibitor-resistant tumors without affecting healthy vessels. Cell 2007; 131: 463-475.
25. Bais C, Wu X, Yao J, Yang S, Crawford Y, McCutcheon K, Tan C, Kolumam G, Vernes JM, Eastham-Anderson J, Haughney P, Kowanetz M, Hagenbeek T, Kasman I, Reslan HB, Ross J, Van Bruggen N, Carano RA, Meng YJ, Hongo JA, Stephan JP, Shibuya M, Ferrara N. PlGF blockade does not inhibit angiogenesis during primary tumor growth. Cell 2010; 141: 166-177.
26. Lieu CH, Tran H, Jiang ZQ, Mao M, Overman MJ, Lin E, Eng C, Morris J, Ellis L, Heymach JV, Kopetz S. The Association of Alternate VEGF Ligands with Resistance to Anti-VEGF Therapy in Metastatic Colorectal Cancer. PLoS One 2013; 8: e77117.
27. Crawford Y, Kasman I, Yu L, Zhong C, Wu X, Modrusan Z, Kaminker J, Ferrara N. PDGF-C mediates the angiogenic and tumorigenic properties of fibroblasts associated with tumors refractory to anti-VEGF treatment. Cancer Cell 2009; 15: 21-34.
28. Ferrara N. Pathways mediating VEGF-independent tumor angiogenesis. Cytokine Growth Factor Rev 2010; 21: 21-26.
29. Li D, Chiu H, Gupta V, Chan DW. Validation of a multiplex immunoassay for serum angiogenic factors as biomarkers for aggressive prostate cancer. Clin Chim Acta 2012; 413: 1506-1511.

統計数理(2014)
第62巻 第1号 3–24

位置情報を用いた疫学研究とその統計的方法

高橋 邦彦[1]・和泉 志津恵[2]・竹内 文乃[3]

(受付 2013年9月20日；改訂 12月10日；採択 12月16日)

要　旨

近年，事象の地理的変動の評価や健康リスクの地域間比較を行うために，収集されるデータに位置情報を付加した空間データの利用が活発になってきている．疫学分野においても，疾病の発生状況の地理的な格差・変動の記述や種々の要因の地理的変動を考慮した検討などを扱う空間疫学研究，空間データをモデルに組み込んだ健康リスクの推定の試み，それらに関連する統計手法が注目されるようになってきている．本稿では空間データを用いたいくつかの疫学研究の事例を紹介し，その中で用いられる方法と研究の進め方について概説する．

キーワード：空間データ，空間疫学，疾病地図，疾病集積性，災害，放射線．

1. はじめに

今日，我々のまわりには様々な数字・データがあふれている．そのなかには系統的に収集されているデータもあるが，その解析などは意図されず，無秩序に収集されてしまっているものもある．たとえば災害時などのデータは乱雑なものも多いが，その中から有用な情報を取り出すことが災害の状況把握やその対策に役立つと考えられる．また新たに集められるものだけではなく，必要に応じてそれまでに報告されている別のデータも併せて利用することで，より有効な情報が得られることもある．なかでも事象の地理的変動や健康リスクの地域間比較を行うために，収集されるデータに位置情報を付加した空間データの利用が近年活発になってきている(矢島, 2012)．またデータから得られた情報や数値は現場や一般市民に広く伝えることが重要であるが，日頃からそれらのデータに接していない者にとっては，その数字を見ただけでは全体を把握することは難しい．そのため地域での空間的な分布の観察や，広域にまたがる大規模災害での状況把握においてはGIS(geographic information system: 地理空間情報システム)の利用も効果的であるが，そこでも位置情報が必要となってくる(Lai et al., 2009)．実際，平成24年(2012年)に改正された災害対策基本法の中でも，災害応急対策ための情報の収集及び伝達等において災害応急対策責任者は「地理空間情報の活用に努めなければならない」「災害に関する情報を共有し，相互に連携して災害応急対策の実施に努めなければならない」と記されるなど，現実社会においても空間情報の利用の重要性が認識されるようになってきている．人間集団における疾病の頻度分布と決定要因についての研究とも定義される疫学研究においても，近年これらの空間データを用いた研究が進んできており，特に疾病の発生状況の地理的な格差・変動を記述したり，種々の要因の地理的変動を考慮した検討，さらにその予兆の早期発見などを扱う空

[1] 名古屋大学大学院 医学系研究科生物統計学分野：〒466–8550 愛知県名古屋市昭和区鶴舞町65
[2] 大分大学 工学部知能情報システム工学科：〒870–1192 大分県大分市旦野原700
[3] 国立環境研究所 環境健康研究センター：〒305–8506 茨城県つくば市小野川16–2

表1. クローン病における全国の2003年度医療受給者証所持者数，死亡数・年齢調整死亡率，ならびに推計された2002年総患者数.

	医療受給者証所持者数（2003年度）	死亡数（2003年）*	年齢調整死亡率（/100万人）（2003年）*	総患者数（2003年）**	受診間隔90日までの者も含めた総患者数（2002年）**
男性	15,436	31	0.39	11,600	16,400
女性	6,904	29	0.34	4,300	5,400

* 土井・横山編（2006）．難病の死亡統計データブック

** 横山・土井編（2008）．平成14年患者調査による難病の受療状況データブック

間疫学研究やそのための統計解析手法も注目されるようになってきている(Waller and Gotway, 2004; Schabenberger and Gotway, 2005; Lawson, 2006; 丹後 他, 2007; Pfeiffer et al., 2008)．しかし実際に空間データを用いた疫学研究を行ったことがある研究者はまだまだ少数であろう．特にこれまで空間データや位置データを扱ったことがない者にとっては，例えば緯度・経度などの情報をどう扱うべきか，またどういうデータが必要になるのかなどがわからず，それが空間データを用いた疫学研究を実施するにあたっての高いハードルになっているのではないかと思われる．

そこで本稿では空間データを用いたいくつかの疫学研究の事例を紹介し，その中で用いられる方法と研究の進め方について概説を行うことで，実際の疫学研究のヒントを与えたい．

2. 疫学研究の事例

本節では空間データを用いた実際の疫学研究の事例として，特定疾患(難病)医療受給者証所持者数の地域比較，大分県内における交通事故発生状況の地域集積性の検討，心肺機能停止傷病者救急搬送件数の時間集積性の検討，ならびに東日本における放射性セシウム曝露量の推計に関する研究を紹介しながら，そこで用いられるデータ，疾病集積性の検定やモデルを用いた推計などの解析手法，結果とその解釈について概説を行う．

2.1 特定疾患(難病)医療受給者証所持者数の地域比較

疾病の発生頻度や患者数の地域比較を行うことは，その疾病の特徴を捉えるうえで大変重要なことである．難病における死亡数の地域比較については，人口動態統計による死亡個票などの行政資料を用いた検討が行われてきた．一方で難病において正確な患者数のデータを把握することは困難であり，これまで全国疫学調査，患者調査をはじめとする標本調査による推計，特定疾患医療受給者証所持者数(以下，所持者数という)などが患者数の目安として用いられ，検討が行われてきている．例えば2003年度クローン病に注目してみると概況は表1のようになっていた．

所持者数は，現在，厚生労働省衛生行政報告例において，全国(対象疾患別，性別，年齢階級別)および都道府県別(対象疾患別，性別)に集計されたデータが公開されており，難病の各研究班においても，患者数に代わる一つの目安として利用されている．一方，平成13年(2001年)～15年(2003年)度においては地域保健・老人保健事業報告において，保健所別の統計表が公開されている．ここでは平成15年(2003年)度全国のクローン病における所持者数を例として，空間疫学的手法を適用した地域比較について検討する(土井 他, 2012)．

2.1.1 疾病地図

今回用いた所持者数は表2のようなデータになっている．なお当該年度のデータでは全国566

表 2. 2003 年度特定疾患医療受給者証所持者数，保健所，性(女)・対象疾病別.

クローン病・女性

保健所	総数	0–9 歳	10–19 歳	20–29 歳	···	60–69 歳	70 歳以上
00 全国	6,904	14	320	1,787	···	551	383
01 北海道	425	1	29	142		18	23
0110 札幌市	159	0	9	53		14	6
0136 小樽市	7	0	0	4		0	0
0137 市立函館	26	0	0	9		1	2
0138 旭川市	37	0	2	12		1	3
0151 江別	11	0	2	2		0	0
⋮							

保健所管轄(ただし京都市は 1 つの保健所として報告)での集計がされていた.

観察データに基づく統計解析を行うにあたっては，まずはそのデータの様子を視覚的に観察することが重要である．一般的なデータでは，最初にヒストグラムや散布図などによってデータの分布の様子を観察すべきであるように，疾病の発生などの空間データにおいてもその分布の様子を把握することは，最も基本的かつ重要なことである.

しかし地域比較を行う場合，単純に観測数のみを考えれば，その数は当然人口の多い地域ほど多くなる傾向がある．また疾病によってはその地域住民の性・年齢構成が影響を与えることもあり，単純に観測数やそれを人口あたりの観測数，また死亡であれば死亡率などだけで比較を行うことは適切ではない．そこで年齢などの影響を取り除くため標準化されたリスク指標を用いた疾病地図がよく利用される．そのためには，まず基準集団(例えば日本全国など)の年齢階級別の発生割合が必要となるが，日本においては国勢調査による人口などが利用できる．表 2 のデータを解析する場合には，簡単のため日本全国を基準集団として 1 番目の年齢階級 0–9 歳で考えると

(日本全国 0–9 歳女性での観測数)/(日本全国 0–9 歳女性の人口)

で 0–9 歳女性の人口あたり所持者数 P_1 が計算できる．これを各年齢階級(表 2 の場合，8 階級)で求める．次に対象となる地域の年齢階級人口データを同様に入手する．今，地域 i での年齢階級 j の人口を $n_j^{(i)}$ としたとき，年齢階級の数を J とすれば

$$e_i = \sum_{j=1}^{J} n_j^{(i)} P_j$$

を地域 i における期待頻度(期待観測数)という．これは「各年齢階級で基準集団と同じ割合で所持者数がいたとすると，この地域では何人の所持者が観測がされると期待されるか」という値になることを意味し，その地域住民の年齢構成を考慮した値となっている.

地域 i の観測数を d_i としたとき，この期待頻度 e_i を用いて

$$SMR_i = d_i/e_i \tag{2.1}$$

を SMR(Standardized Morbidity Ratio)という(観測数が死亡数の場合には Standardized Mortality Ratio として標準化死亡比と呼ばれる．ここでは観測数が所持者数のため Morbidity を用いた)．この SMR を用いた疾病地図は従来からよく用いられているが，それと同時に SMR の指標としての問題点も論じられている．一番の問題は，SMR はその地域の人口の大きさの影響

を受け，特に人口の少ない地域ではSMRの値は不安定になり，人口の異なる市区町村間での地域比較などには適しているとはいえないことである．このことは，その意味する指標を統計学的推測の立場から眺めれば明らかである．いま，地域iの観測数を確率変数D_i，その観測値をd_iとし，ある疾病の発生リスクを基準集団のリスクと比較することを考え，地域iの基準集団に対する相対リスク(relative risk，RR)をθ_iとする．一般に死亡数をはじめ比較的稀な発生事象はPoisson分布に従うと仮定されるので，地域iが基準集団と同じリスク，$\theta_i = 1$，を持てば，地域iでの観測数は基準集団のリスクから計算された期待頻度e_iを期待値とするPoisson分布に従う．もし，地域iが基準集団よりリスクが大($\theta_i > 1$)あるいは小($\theta_i < 1$)であれば観測数の分布は期待頻度$\theta_i e_i$をもつPoisson分布

$$D_i \sim \text{Poisson}(\theta_i e_i) \quad (D_i \text{ と } D_{i'} (i \neq i') \text{ は独立}) \tag{2.2}$$

と仮定できる．そのうえで，相対リスク$(\theta_1, \ldots, \theta_m)$を未知の定数と考え，$\theta_i$の最尤推定量$\hat{\theta}_i$を求めたものが(2.1)式となる．つまり疫学では相対リスクの最尤推定値をSMRと定義しているのである．このことから推定量$\hat{\theta}_i$の標準誤差はe_iに応じて変化することがわかり，市区町村単位など各地域の人口の大きさが大きく異なる場合にはその地域間比較には必ずしも適している指標とは言えなくなる．そのため相対リスク$(\theta_1, \ldots, \theta_m)$をベイズ流に推定する方法がしばしば利用されている．代表的なPoisson-Gammaモデルでは

$$D_i \sim \text{Poisson}(\theta_i e_i), \quad \theta_i \sim \text{Gamma}(\alpha, \beta)$$

と考える．事前分布のパラメータα，βの推定には経験ベイズ法やフルベイズ法などが用いられる．また，さらに複雑なベイズモデルによるリスク指標の推定も行われている(Lawson, 2006, 2013)．

ここでは女性クローン病の所持者数について，日本全国を基準集団としたときの都道府県単位，保健所管轄単位でのSMRのPoisson-Gammaモデルによる経験ベイズ推定値を求め，地図に示した(図1)．また保健所管轄単位での解析においてSMRのベイズ推定値が高い上位10保健所を表3に挙げた．なお保健所管轄の年齢階級別人口は，その管轄に含まれる市区町村の人口を合算したものを用いた．表3のように単純に数値だけの表を見てもなかなか全体を把握できないが，地図に描くことで都道府県でも北海道ならびに九州地方が高い値をとっている様子が把握できる．さらに保健所管轄で細かく見ることで，例えば同じ北海道内でも地域差があることが観察できる．一方で，地図では面積の大きい地域が目立ってしまい，例えば東京周辺はかなり拡大しないと詳細がつかめない．またその階級の決め方や色分けの影響もあり，場合に

表3. SMR(ベイズ推定値)の上位10保健所.

	観測数	期待頻度	SMR(ベイズ推定値) (%)
大分市保健所	45	24.72	148.06
旭川市保健所	37	19.78	146.21
福山市保健所	39	21.87	143.55
徳島保健所	43	24.73	143.27
八日市保健所	24	11.48	143.24
熊本市保健所	61	37.97	141.52
徳山環境保健所	26	13.29	141.30
伊集院保健所	15	5.74	139.87
北九州市保健所	83	54.69	139.22
出雲保健所	19	8.80	138.79

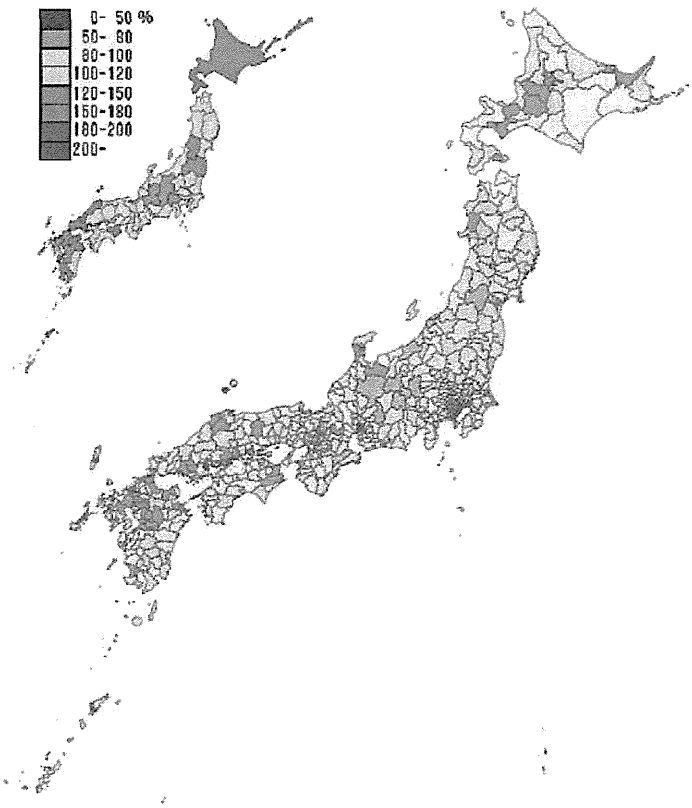

図 1. SMR (経験ベイズ推定値) の疾病地図：都道府県単位(左上)，保健所管轄単位(右)．

よっては誤った印象を与えてしまうこともあるため，結果をみる場合には注意深く観察や考察を行う必要がある．

2.1.2 考察

空間疫学の解析方法を用いた RR の推定とその視覚可である疾病地図によって所持者数の地域分布が異なることを見出すことができた．実際，他の疾患での検討も行ったところ，疾患毎に地域分布が異なる様子が観察できた．また，これらの疾病地図を観察した後，対象としている疾病のリスクの高い地域(もしくは低い地域)が，ある特定の地域に集中しているかどうかを検討する疾病集積性の検定を用いた解析を行うことができる(2.2 節参照)．実際，上記のデータに制限付尤度比に基づく flexible scan statistic(Tango and Takahashi, 2012) (以下，Flexible Scan 法という)を適用して解析を行ったところ，i)久留米保健所を含む 29 保健所($p = 0.0001$)，ii)札幌市保健所を含む 9 保健所($p = 0.0004$)，iii)北九州市保健所を含む 7 保健所($p = 0.0188$)，の 3 つの有意な集積地域が検出された．

一方でここで用いたデータは所持者数であり，厳密な意味での患者数ではなく，それらの間には差異があることも考えられる．この点において，これらの結果の解釈の際には十分な注意が必要であろう．しかし近年，所持者数も年々増加しており，これらのデータを用いた地域比較は有用であると考えられる．今後，関連したデータを用いた，より高度な方法での解析なども検討しながら，これらのデータを有効に活用した解析を行い，その上で，実際の解析結果の解釈について臨床の専門家などと詳細な検討を行うことで，今後の難病研究推進に寄与できるものと考えられる．

2.2 大分県内における交通事故発生状況の地域集積性の検討

交通事故の原因解明や事故防止の対策を立てるうえで，交通事故の第1当事者(犯した過失が，ほかの当事者よりも相対的に重いと判断された当事者)の種別(自動車等，自転車，歩行者)，当事者の年齢や性別，免許取得後の経過年数などの人的特徴とともに，事故発生の日時，地域，天候，などの環境に関する特徴を明らかにすることは重要なことである．全国の交通事故に関する情報は，交通事故分析センター(ITARDA)により都道府県単位や政令指定都市単位のデータがいくつかの項目を掛け合わせた表形式で有償にて配布されている(イタルダ, 2013)．一方，いくつかの都道府県では市区町村単位でまとめられた交通統計も公開されている．

本節では特に大分県内における自動車等(原付以上．以降自動車等と表記)による交通事故に注目し，平成9年(1997年)～18年(2006年)に県内で発生した交通事故の中で，自動車等乗車者の死亡数(交通統計では死者数)の地域比較を行う．データとしては和泉ら(2010)と同様に，大分県内18市町村における調査期間10年間での事故発生市町村別の自動車等乗車者(全年齢)の死者数，免許保有者数を用いる(表4)．なお，ここでの死者数は事故発生後24時間以内での死亡のみがカウントされており，免許保有者数(千人年)は小数点第1位において四捨五入されている．また地域$i(i=1,2,\ldots,18)$の死者数をd_i，免許保有者数をn_iとし，同時期の大分県全体を基準集団として考え，地域iにおける期待頻度e_iやRRを

$$e_i = n_i \times \frac{\sum_{i=1}^{18} d_i}{\sum_{i=1}^{18} n_i}, \qquad RR_i = \frac{d_i}{e_i}$$

として計算し，特に死者数が集中している地域があるか，疾病集積性の検定による検討を行う．

2.2.1 疾病集積性の検定

疾病地図を観察すると，対象としている疾病のリスクの高い地域(もしくは低い地域)が，ある特定の地域に集中しているのではないかと思われることがある．もしこの疾病の発生が集中

表4. 大分県内において発生した人身事故における自動車等(原付以上)乗車者の死者数，免許保有者数，免許保有者10万人対死者数(1997年～2006年)．

	死者数	免許保持者数（千人年）	免許保持者数10万人対死亡者数
大分市	99	2,834	3.5
別府市	14	718	1.9
中津市	36	509	7.1
日田市	43	467	9.2
佐伯市	38	508	7.5
臼杵市	20	280	7.1
津久見市	3	131	2.3
竹田市	11	170	6.5
豊後高田市	18	154	11.7
杵築市	21	199	10.6
宇佐市	52	379	13.7
豊後大野市	31	266	11.7
由布市	25	214	11.7
国東市	25	208	12.0
姫島村	0	14	0.0
日出町	18	163	11.0
九重町	19	70	27.1
玖珠町	12	115	10.4

(集積)しているとすれば，その地域になんらかの原因があるかもしれないし，その疾病が流行性のものであるかもしれない．もし疾病の集積が観察された場合には，集積地域を中心に調査を行い，原因を特定したり対策を講じることが必要となるだろう．しかしこれらの疾病地図だけから「どこかに集積しているか？それとも全体的にばらついているか？」，さらに集積しているとしても「どの範囲までか？」を視覚的に判断するだけでは説得力に欠け，また実際その判断も難しい場合も少なくない．ここに疾病集積性の有無を客観的に決定する分析方法が必要となる．このようなとき「イベントが対象地域内のどこかに集積しているか？」を統計的に検定を行う方法として空間集積性の検定が適用できる．

実際に空間集積性の有無を検出する場合には，研究目的，データの種類(個人ごとの発生情報のような個人単位の点データ，市区町村ごとの発生情報のような地域単位の集計データ)に応じてそれぞれ異なった検定方法が提案されており，それらを使い分ける必要がある(Kulldorff, 2006; Rogerson and Yamada, 2009; Tango, 2010)．空間集積性の検定は，焦点をあてた検定(Focused Test)，一般的な検定(General Test)の2つに分類することがBesag and Newell(1991)によって提案された．焦点をあてた検定は，原子力発電所やごみ焼却施設等の健康に影響を及ぼすと考えられる地点(固定発生源)を中心として，その周辺に空間集積性があるか否かの検定を行う方法である．この方法を用いた代表的な研究事例として，「イタリアにおける高周波無線曝露と白血病疾患との関連性」(Michelozzi et al., 2002)，「日本のごみ焼却施設周辺における週産期健康障害のクラスタ」(Tango et al., 2004)などが挙げられる．検定手法としては，Stone's test(Stone, 1988)，Besag-Newell's test(Besag and Newell, 1991)，スコア検定(Waller et al., 1992; Tango, 1995, 2002)などがある．

一方，一般的な検定は，固定発生源を特定せずに，研究対象領域の中のどこかに空間集積性があるか否かの検討を行う方法である．この一般的な検定は，さらにGlobal Clustering Test (GCT)とCluster Detection Test(CDT)の2つに分けられる．GCTは空間集積性の有無を一般的に検定する方法であり，検定方法としては，点データに対しては，Cuzick-Edward's test (Cuzick and Edward, 1990)，Tango's test(Tango, 2007)が適用可能であり，集計データに対しては，Besag-Newell's test(Besag and Newell, 1991)，Tango's index(Tango, 2000)が適用可能である．この方法を用いた研究事例として，「英国における小児白血病・悪性リンパ腫の空間集積性の検討」(Tango, 2007)などがある．GCTでは統計的に有意な空間集積性があると判断されたとしても，それがどの地域であるかは把握することができない．一方CDTは，空間集積性の有無の検定と同時に空間集積性が認められる地域の位置を検出する方法である．この方法を用いた代表的な研究事例として，「米国北東部の乳がん死亡のクラスタの有無」(Kulldorff et al., 1997)，「英国での新型クロイツフェルト・ヤコブ病のクラスタの有無」(Cousens et al., 2001)などがある．

このCDTにはスキャン統計量を用いた検定がいくつか提案されている．例えば市区町村単位のデータを考える場合，集積(クラスタ)とは1つもしくは複数の市区町村が連結してできる地域と考える．スキャン統計量による検定では，クラスタの候補となる連結した地域のひとつひとつをwindowと呼び，「クラスタが存在する」ということは「観測数が期待観測数に比べ，有意に高くなるwindowが存在する」と考えることができる．逆に「クラスタが存在しない」ということは「全てのwindowについて，その観測数は期待観測数とほぼ同じである」ということになる．前節のSMRの議論と同様，観測数がPoisson分布に従うというPoissonモデルを考える．あるwindow Zを考えて，Zに含まれる地域内のリスクがθ_Zであり，またZの外側の地域ではリスクがθ_{Z^c}であるとする．つまり，全体がm個の地域に分割されているとき，地域$i(i=1,2,\ldots,m)$の観測数D_iが確率変数としてそれぞれ独立に

$$D_i \sim \text{Poisson}(\theta_Z e_i)\ (i \in Z); \qquad D_i \sim \text{Poisson}(\theta_{Z^c} e_i)\ (i \notin Z)$$

であると考え，クラスタの有無は

$$\text{帰無仮説(クラスタ無し)} \quad H_0 : \theta_Z = \theta_{Z^c} \quad (\text{for } {}^{\forall}Z)$$
$$\text{対立仮説(クラスタ有り)} \quad H_1 : \theta_Z > \theta_{Z^c} \quad (\text{for } {}^{\exists}Z)$$

という仮説検定問題を考えることになる．このとき，ひとつひとつの window Z に対して検定を繰り返すと検定の多重性の問題が発生してしまう．そこで Kulldorff and Nagarwalla(1995)，Kulldorff(1997)は尤度比に基づく統計量 $\lambda(Z)$ を考え，ある全体集合 $\mathcal{Z}$ のすべての window $Z(\in \mathcal{Z})$ の中から $\lambda(Z)$ の値が最大のもの(most likely cluster; MLC)を探し，そのときの Z をクラスタの候補とする spatial scan statistic を提案した．このときの尤度比は

$$\lambda(Z) = \begin{cases} \left(\dfrac{d(Z)}{e(Z)}\right)^{d(Z)} \left(\dfrac{d(Z^c)}{e(Z^c)}\right)^{d(Z^c)}, & d(Z) > e(Z) \\ 1, & \text{その他} \end{cases} \tag{2.3}$$

となり，MLC Z^* は $Z^* = \arg\max_{Z \in \mathcal{Z}} \lambda(Z)$ となる．ここで $d(Z)$ は window Z 内全体での観測数，$e(Z)$ は期待頻度とする．MLC として同定された Z^* の有意性の判定については，モンテカルロ検定(Dwass, 1957)が利用される．即ち，各地域の観測事象数を帰無仮説のもとで乱数によって B(たとえば 999 や 9,999)組発生させ，各組の乱数に基づく検定統計量 $\lambda_b = \lambda_b(Z^*)$ $(b = 1, 2, \ldots, B)$ を計算する．一方，実際の観測データに基づく検定統計量を $\lambda^* = \lambda^*(Z^*)$ するとき，p 値の近似値

$$\hat{p} = \frac{1 + \sum_{b=1}^{B} I(\lambda_b \geq \lambda^*)}{B + 1} \qquad I(\cdot) : \text{定義関数}$$

によって有意性の判定を行う．このとき，用いるスキャン統計量や window を構成する際のパラメータによって，帰無仮説のもとでの検定統計量の分布が変化し，p 値も異なってくることに注意する必要がある．

スキャン統計量ではクラスタを探し出す(scan する)window Z の全体集合 $\mathcal{Z}$ のとり方の違いによってもいくつかの統計量が提案されている．Kulldorff and Nagarwalla(1995)，Kulldorff(1997)は，同心円状に，ある限界まで地域を追加していく circular window の全体をとった circular scan statistic(Circular Scan 法)を提案した．$Z_{ik}(k = 1, 2, \ldots, K_i)$ を地域 i から近い順に，i 自身を含む k 個の地域からなる集合とする．ただし各 i の座標はその地域の代表点 1 点(市区町村役場の所在地や人口重心など)であらわすものとする．このとき Circular Scan 法では Z の全体集合として

$$\mathcal{Z}_1 = \{Z_{ik} \mid 1 \leq i \leq m,\ 1 \leq k \leq K_i\} \tag{2.4}$$

を考える．K_i としてはクラスタに含まれる最大距離や人口，最大地域数などが用いられる．この方法は簡便であるが，明らかに円状のクラスタしか同定できない．そこで非円状のクラスタも同定できるよう Circular Scan 法を拡張したいくつかの方法が提案されてきている．たとえば，SA Scan 法(Duczmal and Assunção, 2004)，Upper Level Set(ULS)Scan 法(Patil and Taillie, 2004)，Flexible Scan 法(Tango and Takahashi, 2005)，Echelon Scan 法(栗原・石岡, 2007)などが提案されてきている．これらの方法は非円状の window も同定できるようにしながら，また計算時間が大きくなりすぎないように工夫されている．例えば Flexible Scan 法では，制限された範囲内で非円状のクラスタを同定する方法として，まず地域 i を中心として i 自身を含み i から近い順に K 個の地域からなる集合 Z_{iK} を定める．この Z_{iK} から，i を含み，連結している部

分集合を考え，その全体 $\mathcal{Z}_2$ を考える．つまり Z_{iK} の中で i を含んで k 個の地域からなる連結した window が j_{ik} 個あるとすると，Z の全体集合は

$$\mathcal{Z}_2 = \{Z_{ik(j)} \mid 1 \leq i \leq m,\ 1 \leq k \leq K,\ 1 \leq j \leq j_{ik}\} \tag{2.5}$$

とあらわされる．このため地域の隣接情報(地域が連結している場合 1 となりそうでないとき 0)から定義される隣接行列が必要となる．一方，ULS Scan 法や Echelon Scan 法は距離以外の尺度を用いる．ULS Scan 法では，Flexible Scan 法と同様の隣接行列と事象発生確率を用いて，集積地域の候補となる window を形成する．たとえば地域 i における免許保有者数あたりの死者数を

$$P_i' = (\text{地域 } i \text{ における観測された死者数}) / (\text{地域 } i \text{ における免許保有者数})$$

とし，これを事象発生確率とおく．地域 i を事象発生確率 P_i' の降順に並べ替えたものを i' $(1 \leq i' \leq m)$ とおく．隣接行列の行，列を地域の事象発生確率 P_i' の降順に並び替え，得られた行列の左上から $l \times l$ $(1 \leq l \leq L)$ 行列を取り出す．ただし L は作成される window の最大サイズとする．このとき，この部分行列に含まれる地域の事象発生確率は P_l' 以上となる．$(l-1) \times (l-1)$ 行列までで生成された window 全体を $\mathcal{Z}_{3,l-1}$ とし，そこに含まれる長さ k $(k = 1, 2, \ldots, K_{l-1})$ の window を Z_{kj}' $(j = 1, 2, \ldots, j_{l-1,k})$ とする．$i' = l$ としたとき，地域 i' があるひとつの Z_{kj}' とだけ連結している場合には，$Z_{kj}' \cup i'$ を新たな window とし，いずれの Z_{kj}' とも連結していない場合には i' 自身を window に加える．ただし複数の Z_{kj}' と連結する場合には，i' と連結したものの中で長さが最大となる window だけを候補に加える．また i' によって，複数 Z_{kj}' が連結し 1 つの連結した地域となる場合には，これを新たな window とし，その部分集合は新たな window には加えないものとする．$P_i' \geq P_L'$ までこれを繰り返して与えられたときの Z_{kj}' の全体は

$$\mathcal{Z}_3 = \mathcal{Z}_{3,L} = \{Z_{kj}' \mid 1 \leq k \leq K_L, 1 \leq j \leq j_{L,k}\} \tag{2.6}$$

とあらわされ，これを Upper Level Set という．なお Echelon Scan 法では，ULS Scan 法と同様に，地域の隣接情報と事象発生確率を用いて，エシェロンデンドログラムを描き，それを用いて，集積地域の候補となる window を形成する．

また尤度関数 $\lambda(Z)$ に制約を設けた制約付き尤度比検定(Restricted Likelihood Ratio Test)も提案されている(Tango, 2008; Tango and Takahashi, 2012)．このときの制約付き尤度比は

$$\lambda'(Z) = \begin{cases} \lambda(Z) \cdot I(p_i < \alpha_1), & d(Z) > e(Z) \\ 1, & \text{その他} \end{cases} \tag{2.7}$$

とあらわされる．ここで p_i は帰無仮説 $\theta_i = 1$，対立仮説 $\theta_i \neq 1$ に対する片側 p 値であり，mid-p 値として以下の式で与えられる．

$$p_i = \Pr\{D_i \geq d_i + 1 | D_i \sim \text{Poisson}(e_i)\} + \frac{1}{2}\Pr\{D_i = d_i | D_i \sim \text{Poisson}(e_i)\}.$$

また α_1 は各地域に対しての有意水準として設定されるが，ひとつの目安として $\alpha_1 = 0.20$ が推奨されている(Tango, 2008)．

2.2.2 解析結果

ここでは大分県内における交通事故での自動車等乗車者の死者数について，スキャン統計量を用いた CDT である Circular Scan 法，Flexible Scan 法，ULS Scan 法の 3 つの方法による疾病集積性の検定による解析結果を比較する．Circular Scan 法や Flexible Scan 法を適用する際には，FleXScan V3.1(Takahashi et al., 2012)を利用し，ULS Scan 法を適用する際には統計ソ